Journal of Sound and Vibration 329 (2010) 3520–3536

Contents lists available at ScienceDirect

Journal of Sound and Vibration

journal homepage: www.elsevier.com/locate/jsvi

Coupled vibrations of cantilever cylindrical shells partially submerged in fluids with continuous, simply connected and non-convex domain

E. Askari [a], F. Daneshmand [b,*,1]

[a] Research Department, Samin Sanat Shaigan Company, Isfahan 81966-14996, Iran
[b] Mechanical Engineering Department, School of Engineering, Shiraz University, Shiraz 71348-51154, Iran

ARTICLE INFO

Article history:
Received 4 August 2008
Received in revised form
19 February 2010
Accepted 27 February 2010
Handling Editor: A.V. Metrikine
Available online 1 April 2010

ABSTRACT

The approach developed in the present paper is applied for the coupled-vibration analysis of a cantilever cylindrical shell partially submerged in a fluid with a continuous, simply connected and non-convex domain. The shell is partially and concentrically submerged in a rigid cylindrical container partially filled by a fluid which is assumed to be incompressible and inviscid. The velocity potential for fluid motion is formulated in terms of eigenfunction expansions using the collocation method. The interaction between the fluid and the structure takes into account by using the compatibility requirement along the wet surface of the shell and the Rayleigh–Ritz method is used to calculate natural frequencies and modes of the coupled system. The validity of the developed theoretical method is verified by comparing the results with those obtained from the finite element analysis. Furthermore, the effects of submergence depth, radial distance between shell and container, and circumferential wavenumbers on the natural frequencies and modes of the coupled system are investigated.

1. Introduction

An important class of complex fluid–structure interaction problems involves the introduction of an internal body inside a fluid where the internal body may be partially or completely submerged in the fluid. Therefore, the fluid domain is non-convex, continuous and simply connected. Evans and McIver [1] explored the effect of introducing a vertical baffle into a rectangular container on fluid frequencies. They used the appropriate eigenfunction expansions and solved the resulting integral equation for the fluid on both sides of the baffle. Watson and Evans [2] extended this technique for a number of similar problems. Gavirlyuk et al. [3] developed fundamental solutions of the linearized problem on the fluid sloshing in a vertical cylindrical container having a thin rigid-ring horizontal baffle. A pressure-based finite element technique has been developed to analyze the slosh dynamics of a partially filled rigid container with bottom-mounted submerged components by Mitra and Sinhamahapatra [4]. Maleki and Ziyaeifar [5] investigated the effects of baffles (horizontal ring and vertical blade baffles) in increasing the hydrodynamic damping of sloshing in circular cylindrical storage tanks. All of these

* Corresponding author. Tel.: +98 711 6287508; fax: +98 711 6275028.
E-mail addresses: ehsanaskary@gmail.com (E. Askari), farhang.daneshmand@mcgill.ca, daneshmd@shirazu.ac.ir (F. Daneshmand).
[1] Currently visiting professor, Department of Mechanical Engineering, McGill University, 817 Sherbrooke Street W., Montreal, Québec, Canada H3A 2K6.

0022-460X/$ - see front matter © 2010 Elsevier Ltd. All rights reserved.
doi:10.1016/j.jsv.2010.02.027

Nomenclature

a	container radius
b	internal body radius
B_m	eigenvalue of sth mode of a clamped-free beam
E	Young's modulus
h	internal body length
H	fluid level
$\mathbf{K}^s$	stiffness matrix of the shell
L	container length
$\mathbf{M}^L$	mass matrix of the fluid
$\mathbf{M}^s$	mass matrix of the shell
r, θ, x	longitudinal, circumferential, radial coordinates
$u(x, \theta)$	axial displacement of the shell
$v(x, \theta)$	circumferential displacement of the shell
$w(x, \theta)$	radial displacement of the shell

Greek letters

λ_s	$(2s-1)\pi/2H$
ν	Poison's ratio
ρ_L	mass density of the fluid
ρ_s	mass density of the shell
$\tilde{\varphi}(r,\theta,x,t)$	velocity potential of the fluid
$\varphi^I(r,\theta,x)$	deformation potential in region (I)
$\varphi^{II}(r,\theta,x)$	deformation potential in region (II)
$\psi_m(x)$	beam eigenfunction associated with eigenvalue β_m
ω	circular frequency

researchers obtained some remarkable results for the fluid sloshing in a vertical cylindrical container without considering the fluid–structure interactions.

Cho et al. [6] presented the fluid–structure interaction analysis of fluid-storage containers with baffle, a disc-type baffle with an inner hole, by the structural-acoustic finite element formulation. Ergin and Ugurlu [7] investigated vibration of cantilever plates partially submerged in a fluid using the boundary element method (BEM). Biswal et al. [8] developed a finite element code and investigated the influence of a baffle, a thin annular circular plate, on the dynamic response of a partially fluid-filled cylindrical tank. Esmailzadeh et al. [9] numerically studied dynamic behavior of a 3-D thin flexible structure in an inviscid incompressible stationary fluid. Kerboua et al. [10] developed a numerical approach to consider vibration of rectangular plates totally submerged in a fluid or floating on its free surface.

The problems investigated above can be divided into two major categories. The first one includes the sloshing problems in which the structure and the internal body are assumed to be rigid. In the second category, the interaction between fluid and structure or fluid and internal body are considered by using numerical techniques. In the present paper, the analytical method presented by Evans and McIver [1] for exploring the fluid frequencies without considering the fluid–structure interactions is extended to construct a new analytical method for investigating the problems including the interaction between the fluid and the internal body. For brevity, the project restricts itself to investigate the coupled-vibration of a cantilever cylindrical shell (internal body) partially submerged in a rigid cylindrical container with finite diameter. The submerged cylindrical shell is representative of certain key components of complex structures used in various industries.

In the present paper, attention is focused on the bulging modes of the submerged cylindrical shell. It can be noted that the coupled system has two groups of modes: sloshing and bulging ones [11]. Sloshing modes are caused by the oscillation of the fluid free surface, whereas bulging modes are related to vibrations of the shell. However, the effects of the free surface waves are neglected in the present study. In fact, it is well known that the effect of the free surface waves is low on bulging modes for structures that are not extremely flexible [12].

Generally, the cylindrical shell is a thin-walled and open-ended structure and the Rayleigh–Ritz method is used to derive the characteristic equation of the cantilever cylindrical shell based on Love's thin shell theory. Moreover, the compatibility requirement is applied for the fluid–structure interaction along the contact surface between the shell and the fluid. The bottom plate of the container is flat and rigid, and the fluid is assumed to be incompressible and inviscid. The velocity potential is formulated in terms of eigenfunction expansions for two distinct fluid regions that can be matched across the common vertical boundary (artificial vertical boundary). The resulting equations can be solved by using the collocation method. The present theoretical method for the submerged cylindrical shell is validated by comparing the results with those obtained from the finite element analysis. The effects of the submergence depth, circumferential wavenumbers, axial and radial distances between the shell and the container on the dynamic behavior of the coupled-system are also investigated.

2. Mathematical model

Consider a cantilever cylindrical shell of length h, radius b, and thickness t as shown in Fig. 1. The shell is thin-walled and open-ended, and is assumed to be made of an elastic material with Young's modulus E, Poisson's ratio ν, and mass density ρ_s. The bottom edge of the shell which is partially submerged in a partially fluid-filled cylindrical container is free. The radial, circumferential and axial coordinates are denoted by r, θ and x, respectively. The container is a rigid structure of length L and radius a, and is filled to a height H with an inviscid and incompressible fluid of mass density ρ_L.

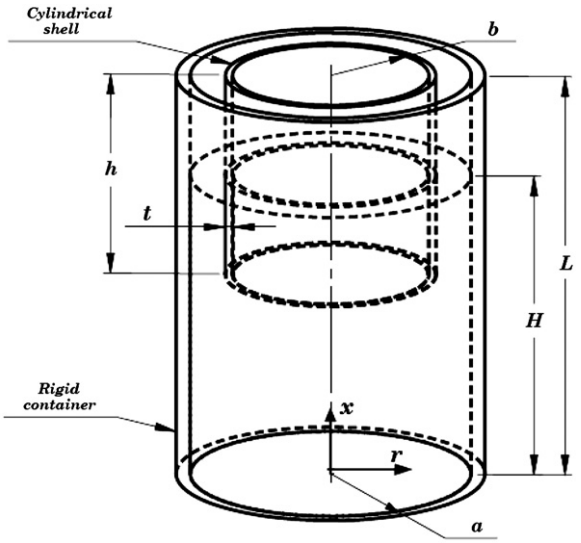

Fig. 1. A concentrically submerged cylindrical shell in a partially fluid-filled rigid container.

2.1. The cylindrical shell

The potential energy for the thin isotropic cylindrical shell is given by [13–15]

$$U_S = \frac{1}{2}\int\int_{\Omega_m}\left[A_s\left(\varepsilon_x^2+2\nu\varepsilon_x\varepsilon_\theta+\varepsilon_\theta^2+\frac{1-\nu}{2}\varepsilon_{x\theta}^2\right)+D_s\left(\kappa_x^2+2\nu\kappa_x\kappa_\theta+\kappa_\theta^2+\frac{1-\nu}{2}\kappa_{x\theta}^2\right)\right]b\,\mathrm{d}x\,\mathrm{d}\theta \tag{1}$$

where coefficients A_s and D_s are stretching and bending stiffness of the shell, respectively, and Ω_m is the shell middle surface.

$$A_s=\frac{Et}{1-\nu^2},D_s=\frac{Et^3}{12(1-\nu^2)} \tag{2}$$

From Love's thin shell theory, the strain and curvature ε_i, κ_i, $i=x,\theta,x\theta$ in the middle shell surface are as follows for $n>0$ [13–15]

$$\varepsilon_x=\frac{\partial u}{\partial x},\varepsilon_\theta=\frac{1}{b}\left(\frac{\partial v}{\partial\theta}+w\right),\varepsilon_{x\theta}=\frac{\partial u}{b\partial\theta}+\frac{\partial v}{\partial x},$$

$$\kappa_x=-\frac{\partial^2 w}{\partial x^2},\kappa_\theta=-\frac{1}{b^2}\left(\frac{\partial^2 w}{\partial\theta^2}-\frac{\partial v}{\partial\theta}\right),\kappa_{x\theta}=-\frac{1}{b}\left(2\frac{\partial^2 w}{\partial x\partial\theta}-\frac{\partial v}{\partial x}\right) \tag{3}$$

where u, v, and w are axial, circumferential and radial displacements of the shell on the shell middle surface, respectively. For the axisymmetric case (n=0), all derivatives with respect to θ vanish.

The reference kinetic energy of the shell is given by [13–15]

$$T_S^*=\frac{1}{2}\rho_s t\int\int_{\Omega_m}[(u(x,\theta)^2+v(x,\theta)^2+w(x,\theta)^2]b\,\mathrm{d}x\,\mathrm{d}\theta \tag{4}$$

The Rayleigh–Ritz method is applied to find natural modes of the cylindrical shell, and the time variation is assumed to be harmonic. The admissible displacement functions for the free vibration of the cylindrical shell with any boundary condition can be written as [15,16]

$$u(x,\theta)=\sum_{m=1}^{\infty}U_{mn}\frac{1}{\alpha_m}\frac{\partial\Psi_m(x)}{\partial x}\cos(n\theta),\alpha_m=\frac{\beta_m}{h}$$

$$v(x,\theta)=\sum_{m=1}^{\infty}V_{mn}\Psi_m(x)\sin(n\theta)$$

$$w(x,\theta)=\sum_{m=1}^{\infty}W_{mn}\Psi_m(x)\cos(n\theta) \tag{5}$$

where U_{mn}, V_{mn} and W_{mn} are the Ritz unknown coefficients and m and n are axial half-wave and circumferential wavenumbers. $\Psi_m(x)$ is used as the admissible function that is the in vacuo beam function, satisfying the imposed boundary conditions. It has been shown by Blevins [17] that the choice of the beam functions as the test functions is appropriate provided that the ratio of the shell length to its radius is greater than eight.

In the present article, the cylindrical shell with clamped-free boundary conditions (clamped at $x=L$ and free at $x=L-h$) is considered. Therefore, $\Psi_m(x)$ is given by

$$\Psi_m(x)=\left(\cosh\left(\frac{\beta_m}{h}(L-x)\right)-\cos\left(\frac{\beta_m}{h}(L-x)\right)\right)-\sigma_m\left(\sinh\left(\frac{\beta_m}{h}(L-x)\right)-\sin\left(\frac{\beta_m}{h}(L-x)\right)\right)$$

$$\sigma_m=\frac{\cosh(\beta_m)+\cos(\beta_m)}{\sinh(\beta_m)+\sin(\beta_m)} \tag{6}$$

where β_m are solutions of the following equation:

$$\cosh(\beta_m)\cos(\beta_m)+1=0 \tag{7}$$

2.2. Dynamic behavior of the fluid–structure interaction

The usual linearized theory of water wave permits the introduction of a velocity potential for the fluid motion. Assuming simple harmonic motion of circular frequency ω, the velocity potential can be expressed as

$$\tilde{\varphi}(r,\theta,x,t)=\mathrm{i}\omega\varphi(r,\theta,x)\mathrm{e}^{\mathrm{i}\omega t},\mathrm{i}^2=-1 \tag{8}$$

The fluid domain is continuous, simply connected and non-convex. In order to compute the time-independent velocity potential, $\varphi(r,\theta,x)$, the fluid domain can be divided into two parts (I) and (II) as shown in Fig. 2, [1,2].

$$I=\{(r,\theta,x):0\le x\le H,r<b\}\ \text{ and }\ II=\{(r,\theta,x):0\le x\le H,b<r<a\} \tag{9}$$

The fluid deformation potential in two regions is assumed to be of the form below [1,2,18]:

$$\varphi^I=\sum_{m=1}^{\infty}W_{mn}\varphi^I_{mn},\ \varphi^{II}=\sum_{m=1}^{\infty}W_{mn}\varphi^{II}_{mn} \tag{10}$$

where φ^I and φ^{II} are time-independent velocity potentials in regions (I) and (II), respectively, and φ^I_{mn} and φ^{II}_{mn} are eigenfunctions.

It will be convenient to define

$$\gamma=\{(r,\theta,x):r=b,0<\theta<2\pi,x<L-h\},\ \gamma'=\{(r,\theta,x):\ r=b,0<\theta<2\pi,L-h<x<H\} \tag{11}$$

where γ is boundary between two fluid regions and γ' is contact boundary between the fluid and the cylindrical shell. The fluid along the boundary γ' is in contact with inner and outer of the lateral cylindrical shell for regions (I) and (II), respectively.

We consider region (I) to find function$\varphi^I(r,\theta,x)$. This function satisfies conditions (12)–(15) in that region and the condition $\varphi^I=0$ on $r=0$. For an inviscid and incompressible fluid with an irrotational movement due to the structural vibration (quiescent fluid), the potential φ^I satisfies the Laplace equation, so

$$\nabla^2\varphi^I=0 \tag{12}$$

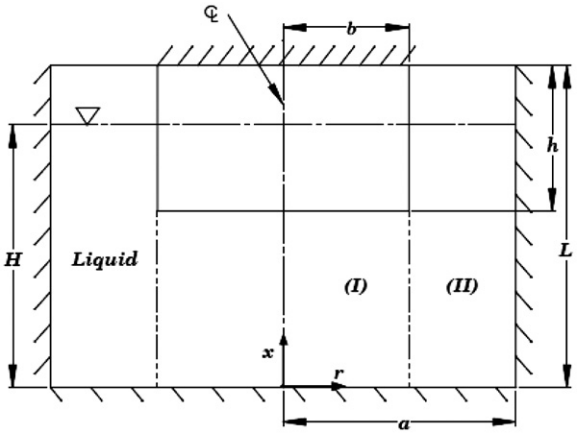

Fig. 2. Geometry of the submerged cylindrical shell in the partially fluid-filled rigid container and coordinate systems.

For stationary fluid, the radial velocities of fluid and cylindrical shell must be equal along γ'. This is the contact condition when there is no cavitation along the interface [19]. Therefore

$$\frac{\partial \varphi^I}{\partial r} = w,\ r = b,\ L-h < x < H \tag{13}$$

When the fluid is in contact with the rigid bottom of the container, the fluid velocity in the vertical direction should be zero,

$$\frac{\partial \varphi^I}{\partial x} = 0, x = 0 \tag{14}$$

$$\frac{\partial \tilde{\varphi}^I}{\partial t} = 0 \Rightarrow \varphi^I = 0,\ x = H \tag{15}$$

where $\tilde{\varphi}^I$ is the velocity potential in region (I). This condition states that the pressure on the free surface in region (I) is zero.

In the inner fluid region (I), using the method of separation of variables gives

$$\varphi^I_{mn} = \cos(n\theta) \sum_{s=1}^{\infty} A_{mns} \cos(\lambda_s x) I_n(\lambda_s r),\ \lambda_s = (2s-1)\frac{\pi}{2H}, s = 1,2,3,\ldots \tag{16}$$

which satisfies conditions (12), (14) and (15), and also vanishes on r=0 as required. I_n is the modified Bessel function of the first kind of order n.

Now, we consider region (II) and seek function $\varphi^{II}(r,\theta,x)$, satisfying conditions (17)–(21) in that region.

For an inviscid, incompressible fluid with an irrotational movement due to the structural vibration (quiescent fluid), the potential φ^{II} satisfies the Laplace equation, so

$$\nabla^2 \varphi^{II} = 0 \tag{17}$$

The radial velocities of the fluid and the cylindrical shell must be equal along γ'. This is the contact condition between an impermeable shell and a fluid when there is no cavitation along the interface [19]. Therefore

$$\frac{\partial \varphi^{II}}{\partial r} = w,\ r = b,\ L-h < x < H \tag{18}$$

For the fluid in contact with the rigid bottom of the container, the fluid velocity in the vertical direction should be zero, so

$$\frac{\partial \varphi^{II}}{\partial x} = 0,\ x = 0 \tag{19}$$

$$\frac{\partial \tilde{\varphi}^{II}}{\partial t} = 0 \Rightarrow \varphi^{II} = 0,\ x = H \tag{20}$$

where $\tilde{\varphi}^{II}$ is velocity potential in region (II). It means that the pressure on the free surface in region (II) is zero. For the fluid in contact with the lateral rigid wall of the container, the fluid velocity in the radial direction is zero, so

$$\frac{\partial \varphi^{II}}{\partial r} = 0\ \ r = a,\ 0 < x < H \tag{21}$$

In the outer fluid region (II), the method of separation of variables gives

$$\varphi^{II}_{mn} = \cos(n\theta) \sum_{s=1}^{\infty} B_{mns} \cos(\lambda_s x) \left[I_n(\lambda_s r) - \frac{I'_n(\lambda_s a)}{K'_n(\lambda_s a)} K_n(\lambda_s r) \right], \lambda_s = (2s-1)\frac{\pi}{2H}, s = 1,2,3,\ldots \tag{22}$$

where K_n is the modified Bessel function of the second kind of order n, and I'_n and K'_n indicate the derivatives of I_n and K_n, with respect to r. φ^{II}_{mn} satisfies the boundary conditions (17), (19)–(21). A_{mns} and B_{mns} are unknown coefficients to be determined by the matching process, depending on the integers m, n and s. It is also necessary to ensure that the potentials and velocities of fluid are continuous along γ, and the conditions (13) and (18) are satisfied along γ'. These conditions are presented in Eqs. (23), (24a) and (24b) as follows:

$$\frac{\partial \varphi^I}{\partial r}(r = b) = \begin{cases} \dfrac{\partial \varphi^{II}}{\partial r}(r = b) & \text{on } \gamma \\ \omega & \text{on } \gamma' \end{cases} \tag{23}$$

Eq. (23) indicates that the radial velocity of the fluid is continuous along γ. The radial velocity of the fluid is equal to the radial velocity of the cylindrical shell in region (I) and along γ'.

The continuity condition for the velocity potentials along boundary γ requires that

$$\varphi^{II} = \varphi^I \ \text{ on } \gamma \tag{24a}$$

The radial velocity of the fluid is equal to the radial velocity of the cylindrical shell along γ' and in region (*II*), so

$$\frac{\partial \varphi^{II}}{\partial r}(r=b)=w \ \text{ on } \gamma' \tag{24b}$$

Eq. (23) must be satisfied for all values $0\le x\le H$ (on boundary, $\gamma+\gamma'$). If one applies the collocation method on this equation, one obtains

$$\mathbf{QA}_{mn}=\mathbf{RB}_{mn}+\mathbf{S}$$

$$\begin{cases}\mathbf{Q}_{js}=I'_n(\lambda_s b)\cos(\lambda_s x_j)\\ \mathbf{R}_{js}=\left[I'_n(\lambda_s b)-\dfrac{I'_n(\lambda_s a)}{K'_n(\lambda_s a)}K'_n(\lambda_s b)\right]\cos(\lambda_s x_j) & \text{on } \gamma\\ \mathbf{S}_j=0\end{cases}$$

$$\begin{cases}\mathbf{Q}_{js}=I'_n(\lambda_s b)\cos(\lambda_s x_j)\\ \mathbf{R}_{js}=0 & \text{on } \gamma'\\ \mathbf{S}_j=\psi_m(x_j)\end{cases}$$

$$\mathbf{A}_{mn}=\begin{Bmatrix}A_{mn1}\\ \vdots\\ A_{mns}\end{Bmatrix},\ \mathbf{B}_{mn}=\begin{Bmatrix}B_{mn1}\\ \vdots\\ B_{mns}\end{Bmatrix}\ x_j=(j-1)\frac{H}{N},\ j=1,\ldots,N \tag{25}$$

where x_j is selected as points used in the collocation method. Eqs. (24a) and (24b) must be satisfied for all values $0\le x\le H$ (on boundary, $\gamma+\gamma'$). If one applies the collocation method on these equations, one obtains

$$\mathbf{TB}_{mn}=\mathbf{OA}_{mn}+\mathbf{P}$$

$$\begin{cases}\mathbf{T}_{js}=\left(I_n(\lambda_s b)-\dfrac{I'_n(\lambda_s a)}{K'_n(\lambda_s a)}K_n(\lambda_s b)\right)\cos(\lambda_s x_j)\\ \mathbf{O}_{js}=I_n(\lambda_s b)\cos(\lambda_s x_j) & \text{on } \gamma\\ \mathbf{P}_j=0\end{cases}$$

$$\begin{cases}\mathbf{T}_{js}=\left(I'_n(\lambda_s b)-\dfrac{I'_n(\lambda_s a)}{K'_n(\lambda_s a)}K'_n(\lambda_s b)\right)\cos(\lambda_s x_j)\\ \mathbf{O}_{js}=0 & \text{on } \gamma'\\ \mathbf{P}_j=\Psi_m(x_j)\end{cases}$$

$$\mathbf{A}_{mn}=\begin{Bmatrix}A_{mn1}\\ \vdots\\ A_{mns}\end{Bmatrix},\ \mathbf{B}_{mn}=\begin{Bmatrix}B_{mn1}\\ \vdots\\ B_{mns}\end{Bmatrix}\ x_j=(j-1)\frac{H}{N},\ j=1,\ldots,N \tag{26}$$

where x_j is selected as points used in the collocation method. The coefficients A_{mns} and B_{mns} are computed by solving the following equations:

$$\begin{cases}\mathbf{QA}_{mn}=\mathbf{RB}_{mn}+\mathbf{S}\\ \mathbf{TA}_{mn}=\mathbf{OB}_{mn}+\mathbf{P}\end{cases} \tag{27}$$

The Rayleigh–Ritz method is used to calculate the natural frequencies and mode shapes. It is useful to introduce the Rayleigh quotient [20,21] for the system considered, which is

$$\omega^2=\frac{U_S}{T_S^*+T_L^*} \tag{28}$$

where U_S and T_S^* are defined in Eqs. (1) and (4), respectively. The only term that remains to be computed in Eq. (28) is the simplified reference kinetic energy of the fluid, T_L^*, which, by using Green's theorem [18,19], is

$$T_L^*=\frac{1}{2}\rho_L\int\int_{\Omega}\varphi^{II}\frac{\partial\varphi^{II}}{\partial\mathbf{z}}b\,\mathrm{d}x\,\mathrm{d}\theta+\int\int_{\Omega_1}\varphi^{I}\frac{\partial\varphi^{I}}{\partial\mathbf{z}}b\,\mathrm{d}x\,\mathrm{d}\theta \tag{29}$$

where Ω and Ω_1 are the outer and inner surface of the shell in contact with the fluid, respectively, and $\mathbf{z}$ is normal direction at any point on the boundary surface of the fluid domain ($\Omega\cup\Omega_1$) pointing outwards, ($\mathbf{z}$=r on Ω_1; $\mathbf{z}$=r on Ω). By

substituting Eqs. (12) and (18) in Eq. (29), we can write

$$T_L^* = \frac{1}{2}\rho_L \int_0^{2\pi} \int_{L-h}^{H} (-\varphi^{II} + \varphi^{I})_{r=b} wb \, dx \, d\theta \tag{30}$$

2.3. The eigenvalue problem

For the numerical calculation of natural frequencies and Ritz unknown coefficients, only M terms in the expansion of u, v and w, Eq. (5), and N in the expansion of φ_{mn}^{I} and φ_{mn}^{II}, Eqs. (16) and (22) are considered, where M and N are chosen large enough to give the required accuracy. Therefore, all the energies are given by finite summations. It is convenient to introduce a vectorial notation. The vector $\mathbf{q}$ of the parameters of the Ritz expansion is defined by

$$\mathbf{q} = \begin{Bmatrix} \mathbf{U} \\ \mathbf{V} \\ \mathbf{W} \end{Bmatrix}, \mathbf{U} = \begin{Bmatrix} U_{1n} \\ \vdots \\ U_{Mn} \end{Bmatrix}, \mathbf{V} = \begin{Bmatrix} V_{1n} \\ \vdots \\ V_{Mn} \end{Bmatrix}, \mathbf{W} = \begin{Bmatrix} W_{1n} \\ \vdots \\ W_{Mn} \end{Bmatrix} \tag{31}$$

The maximum potential energy of the shell, Eq. (1), becomes

$$U_S = \tfrac{1}{2}\vartheta_n \mathbf{q}^T \mathbf{K}^s \mathbf{q} \tag{32}$$

where $\vartheta_n = \pi$ for $n > 0$ and $\vartheta_n = 2\pi$ for n=0, the partitioned matrix $\mathbf{K}^s$ is

$$\mathbf{K}^s = \begin{bmatrix} \mathbf{K}^{11} & \mathbf{K}^{12} & \mathbf{K}^{13} \\ \mathbf{K}^{21} & \mathbf{K}^{22} & \mathbf{K}^{23} \\ \mathbf{K}^{31} & \mathbf{K}^{32} & \mathbf{K}^{33} \end{bmatrix} \tag{33}$$

where the elements of the submatrices $\mathbf{K}^{kl}$, (k,l=1,2,3) are given by

$$\mathbf{K}_{ij}^{11} = \frac{A_s}{\alpha_i \alpha_j}\left[b \int_{L-h}^{L} \frac{\partial^2 \Psi_i}{\partial x^2} \frac{\partial^2 \Psi_j}{\partial x^2} \, dx + (1-\nu)\frac{n^2}{2b} \int_{L-h}^{L} \frac{\partial \Psi_i}{\partial x} \frac{\partial \Psi_j}{\partial x} \, dx \right], i,j = 1, \ldots, M$$

$$\mathbf{K}_{ij}^{12} = \frac{A_s n}{2\alpha_i}\left[2\nu \int_{L-h}^{L} \frac{\partial^2 \Psi_i}{\partial x^2} \psi_j \, dx - (1-\nu) \int_{L-h}^{L} \frac{\partial \Psi_i}{\partial x} \frac{\partial \Psi_j}{\partial x} \, dx \right]$$

$$\mathbf{K}_{ij}^{13} = \frac{A_s \nu}{\alpha_i} \int_{L-h}^{L} \frac{\partial^2 \Psi_i}{\partial x^2} \psi_j \, dx$$

$$\mathbf{K}_{ij}^{22} = \left(A_s b \frac{1-\nu}{2} + D_s \frac{1-\nu}{2b} \right) \int_{L-h}^{L} \frac{\partial \Psi_i}{\partial x} \frac{\partial \Psi_j}{\partial x} \, dx + \left(D_s \frac{n^2}{b^3} + A_s \frac{n^2}{b} \right) \int_{L-h}^{L} \Psi_i \Psi_j \, dx$$

$$\mathbf{K}_{ij}^{23} = \left(A_s \frac{n}{b} + D_s \frac{n^3}{b^3} \right) \int_{L-h}^{L} \Psi_i \Psi_j \, dx + D_s \left[n \left(\frac{1-\nu}{b} \int_{L-h}^{L} \frac{\partial \Psi_i}{\partial x} \frac{\partial \Psi_j}{\partial x} \, dx - \frac{\nu}{b} \int_{L-h}^{L} \frac{\partial^2 \Psi_i}{\partial x} \psi_j \, dx \right) \right]$$

$$\mathbf{K}_{ij}^{33} = \frac{A_s}{b} \int_{L-h}^{L} \Psi_i \Psi_j \, dx + D_s \left[b \int_{L-h}^{L} \frac{\partial^2 \Psi_i}{\partial x^2} \frac{\partial^2 \Psi_j}{\partial x^2} \, dx - 2\nu \frac{n^2}{b} \int_{L-h}^{L} \frac{\partial^2 \Psi_i}{\partial x^2} \psi_j \, dx + \frac{n^4}{b^3} \int_{L-h}^{L} \Psi_i \Psi_j \, dx + 2n^2 \frac{1-\nu}{b} \int_{L-h}^{L} \frac{\partial \Psi_i}{\partial x} \frac{\partial \Psi_j}{\partial x} \, dx \right]$$

$$\mathbf{K}_{ij}^{21} = \mathbf{K}_{ji}^{12}, \mathbf{K}_{ij}^{31} = \mathbf{K}_{ji}^{13}, \mathbf{K}_{ij}^{32} = \mathbf{K}_{ji}^{23} \tag{34}$$

The reference kinetic energy of the shell, Eq. (4), may be written as

$$T_S^* = \tfrac{1}{2}\vartheta_n \mathbf{q}^{\mathrm{T}} \mathbf{M}^s \mathbf{q} \tag{35}$$

where

$$\mathbf{M}^s = \begin{bmatrix} \mathbf{M}^{11} & \mathbf{0} & \mathbf{0} \\ \mathbf{0} & \mathbf{M}^{22} & \mathbf{0} \\ \mathbf{0} & \mathbf{0} & \mathbf{M}^{33} \end{bmatrix} \tag{36}$$

where the elements of the submatrices $\mathbf{M}^{kk}$,($k = 1,2,3$) are given by

$$\mathbf{M}_{ij}^{11} = b\rho_s t \int_{L-h}^{L} \frac{1}{\alpha_i \alpha_j} \frac{\partial \Psi_i}{\partial x} \frac{\partial \Psi_j}{\partial x} \, dx$$

$$\mathbf{M}_{ij}^{22} = \mathbf{M}_{ij}^{33} = b\rho_s t \int_{L-h}^{L} \Psi_i(x) \Psi_j(x) \, dx, i,j = 1 \ldots M \tag{37}$$

The simplified reference kinetic energy of the fluid, Eq. (30), can be written as

$$T_L^* = \tfrac{1}{2}\vartheta_n \mathbf{q}^{\mathrm{T}} \mathbf{M}^L \mathbf{q} \tag{38}$$

where $\vartheta_n = \pi$ for $n > 0$ and $\vartheta_n = 2\pi$ for n=0, which

$$\mathbf{M}^L = \begin{bmatrix} \mathbf{0} & \mathbf{0} & \mathbf{0} \\ \mathbf{0} & \mathbf{0} & \mathbf{0} \\ \mathbf{0} & \mathbf{0} & \mathbf{M}^F \end{bmatrix} \tag{39}$$

The elements of submatrix $\mathbf{M}^F$ can be written as

$$\mathbf{M}_{ij}^F = b\rho_L \sum_{s=1}^{N} \int_{L-h}^{H} \cos(\lambda_s x)\Psi_j(x)\,\mathrm{d}x \times \left(-B_{ins}\left(I_n(\lambda_s b) - \frac{I_n'(\lambda_s a)}{K_n'(\lambda_s a)} K_n(\lambda_s b)\right) + A_{ins} I_n(\lambda_s b) \right), i,j = 1 \ldots M \tag{40}$$

Substituting Eqs. (32), (35) and (38) into the Rayleigh quotient, Eq. (28), and then minimizing with respect to the coefficients $\mathbf{q}_i$, we obtain

$$\mathbf{K}^s \mathbf{q} - \omega^2 (\mathbf{M}^s + \mathbf{M}^L)\mathbf{q} = 0 \tag{41}$$

where ω is the circular frequency of the submerged cylindrical shell. Eq. (41) gives a linear eigenvalue problem for a real, non-symmetric matrix.

$$(\mathbf{Q} - \omega^2 \mathbf{I})\mathbf{q} = 0, \mathbf{Q} = (\mathbf{M}^s + \mathbf{M}^L)^{-1}\mathbf{K}^s \tag{42}$$

For the axisymetric case, n=0, the torsional mode decouples and rendering the matrix $\mathbf{Q}$ given in Eq. (42) block diagonal. Thus, it can be dealt with independent of the radial and longitudinal motions. These results in two independent matrix equations: one involving a $M \times M$ coefficient matrix for the torsion problem and the second involving a $2M \times 2M$ coefficient matrix corresponding to the other modes. The product of the determinants of these two coefficient matrices gives the frequency equation for the axisymmetric modes.

3. Results and discussions

Based on the preceding analysis, the eigenvalue problem, Eq. (41), is solved to find the natural frequencies and mode shapes of a submerged cylindrical shell. To check the validity and accuracy of the proposed method, the comparisons are made with FEM results. In the finite element analysis, the 2-D axisymmetric model is constructed with the axisymmetric structural shell element for the elastic structure and the axisymmetric fluid element or the fluid region. The shell element is defined by two nodes having four degrees of freedom at each node: three translations in each direction and one rotation. The geometry, node locations, and the coordinate systems for this element are shown in Fig. 3. The fluid element is defined by four nodes having three degrees of freedom at each node: three translations in each direction [22]. The geometry, node locations, and the coordinate systems for this element are shown in Fig. 4. The radial velocities of the fluid nodes along the wet surface of the cylindrical shell coincide with the corresponding velocities of the cylindrical shell. The radial velocities of the fluid nodes along the wet surface of the container are zero. In the present paper, the effects of the free surface waves are neglected. Consequently, the time-independent velocity potential of the fluid nodes on the free surface in two regions (I, II) is zero. In the present finite element model, the shell is divided into 90 2-D axisymmetric structural shell elements of the same size, whereas the fluid region consists of 2430 fluid elements as illustrated in Fig. 5.

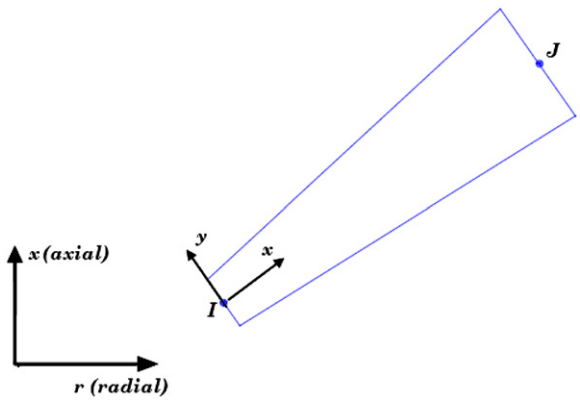

Fig. 3. Shell element: geometry, node locations, and coordinate system.

The following material properties are used: the shell is made of steel with Young's modulus E=206 GPa, Poisson's ratio v=0.3 and mass density ρ_s=7850 kg/m^3; the fluid is water with mass density ρ_L=1000 kg/m^3. The rigid container is partially filled to H=0.67L and its dimensions are a=1.1b with length L=6b for case 1 and a=1.3b with same length for case 2. The cylindrical shell dimensions are b=0.1 m, h=0.75L, and t=0.002 m.

3.1. Convergence and validity study

To check the convergence of the developed method, a cylindrical shell with clamped-free boundary conditions submerged in a partially fluid-filled cylindrical container (case 1) is analyzed. Both Tables 1 and 2 present the convergence of the developed method for different number of terms in the series expansions. It is seen that 10 shell modes (M=10) in the Ritz expansion, and 25 terms (N=25) in the expansion of φ^I_{mn} and φ^{II}_{mn} are enough to give a good accuracy.

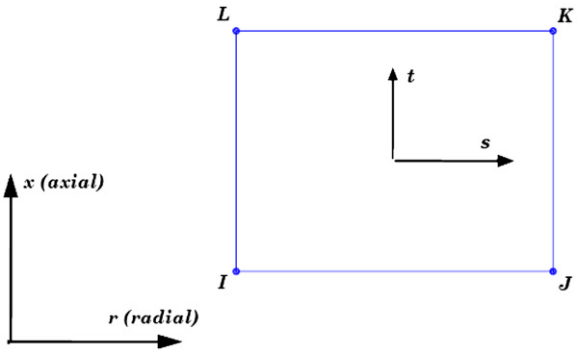

Fig. 4. Fluid element: geometry, node locations, and coordinate system.

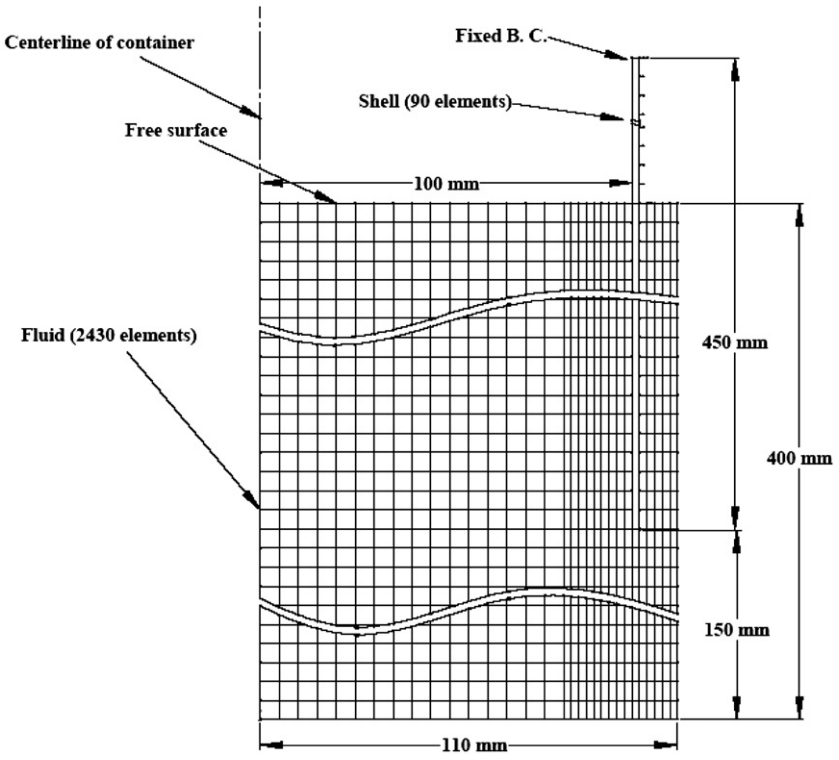

Fig. 5. Finite element model for a cylindrical shell submerged in a cylindrical rigid container.

To validate the developed theoretical method, the results for the partially submerged cylindrical shell in cases 1 and 2 are compared with those obtained from the finite element analysis, in Table 3. The results are in good agreement, whereas the largest discrepancy is <2.5 percent and 4 percent for cases 1 and 2, respectively. As it is mentioned in Section 2, using the beam functions is satisfactory if (h/b) is greater than eight. This ratio is 4.5 for the present particular case and nevertheless, the results obtained from the mathematical model are in good agreement with those of the numerical ones. It should be noted that in general, the use of beam functions represents an approximation which is expected to break-down for shells with smaller length-to-radius ratios. Moreover, a formulation is prepared for considering the first uncoupled acoustic frequencies of the fluid system. It should be noted that the solution of the problem is obtained by an iterative algorithm. It is seen that the assumption of incompressibility may have some errors for frequencies larger than 1000 Hz and the effects of compressibility cannot be ignored for these frequencies.

Table 1
Convergence study of natural frequencies (Hz), effect of the series terms M with N=25.

Mode no.		M				
n	m	4	6	8	10	12
2	1	95.13	94.69	94.49	94.36	94.30
	2	645.58	629.76	628.03	626.20	625.98
3	1	143.34	143.24	143.20	143.16	143.14
	2	427.27	421.63	420.96	420.20	420.06
4	1	299.03	299.00	298.96	298.95	298.95
	2	459.14	455.60	455.37	455.02	454.96
5	1	538.80	538.78	538.69	538.68	538.66
	2	659.48	653.28	652.91	652.52	652.36
6	1	865.24	865.23	865.09	865.08	865.07
	2	972.41	959.19	958.65	957.99	957.89

Table 2
Convergence study of natural frequencies (Hz), effect of the series terms N with M=10.

Mode no.		N					
n	m	10	15	19	22	25	28
2	1	88.06	90.79	94.23	94.30	94.36	94.33
	2	590.07	603.88	626.13	626.12	626.20	626.26
3	1	137.40	139.64	143.01	143.09	143.16	143.22
	2	406.61	410.10	420.28	420.19	420.20	420.26
4	1	291.55	294.08	298.64	298.80	298.95	299.08
	2	447.29	447.63	455.01	454.97	455.02	455.01
5	1	531.23	533.31	538.19	538.45	538.68	538.76
	2	645.00	644.33	652.01	652.24	652.52	652.80
6	1	859.13	860.17	864.40	864.77	865.08	865.15
	2	951.31	949.49	956.81	657.40	957.99	958.31

Table 3
Coupled natural frequencies (Hz) of the partially submerged cylindrical shell.

Mode no.	m	n	Case 1 (a=0.11 m)		Case 2 (a=0.13 m)	
			FEM (ANSYS)	This study	FEM (ANSYS)	This study
1st	1	2	94.03	94.36	125.81	126.53
2nd	1	3	140.23	143.16	177.33	181.42
3rd	1	1	196.21	200.48	274.40	282.65
4th	1	4	291.54	298.95	351.56	360.95
5th	2	3	415.49	420.20	499.41	506.98
6th	2	4	444.55	455.02	520.07	532.13
7th	1	5	528.32	538.68	612.27	625.38
8th	2	5	640.48	652.52	735.89	744.35
9th	2	2	618.54	626.20	770.69	783.76
10th	1	6	852.00	865.08	959.29	972.88

3.2. Effect of the container radius

In order to study the effect of the radial distance between the shell and the container on the dynamic characteristics of the coupled system, the radius ratio is defined as

$$R_{ab} = \left(\frac{a}{b}\right),\ 1 < R_{ab} < \infty \tag{43}$$

Moreover, a normalized natural frequency is defined as the coupled natural frequency divided by the natural frequency of the submerged shell with infinite radius ratio for the specific corresponding mode.

Fig. 6 shows the normalized natural frequencies of the submerged cylindrical shell as a function of radius ratio R_{ab}, for various axial half-wave and circumferential wavenumbers. As it can be observed from Fig. 6, the normalized natural frequencies increase with increasing radius ratio. Fig. 6-a illustrates that the natural frequency of the shell can be reduced by about 60 percent for $n=1$, $m=1$, and $R_{ab}\sim 1$. This reduction is due to interaction between the container and the submerged shell through the fluid. The natural frequencies of the shell rapidly converge to those obtained for the shell submerged in an unbounded liquid in the radial direction. As can be seen from Fig. 6, it occurs about radius ratio 2.5. In fact, the container has a small effect on the vibrating shell when its distance to the internal body is large enough. The same conclusion has also been reported in some references [24,25]. As can be seen from Fig. 6, the variations of the normalized frequencies of the submerged shell with radius ratio also depend on the axial half-wave and circumferential wavenumbers. In fact, the normalized natural frequencies increase with increasing the circumferential mode number. If the radius ratio approaches unity, the normalized natural frequencies decrease dramatically since the narrow annular gap, the distance between the submerged shell and the container, produces a great hydrodynamic mass due to a lengthened moving length of the fluid. That is to say, the narrow annular gap works as a one directional channel carrying fluid during vibration, which produces an increased added mass, and eventually reduces the natural frequencies of the shell.

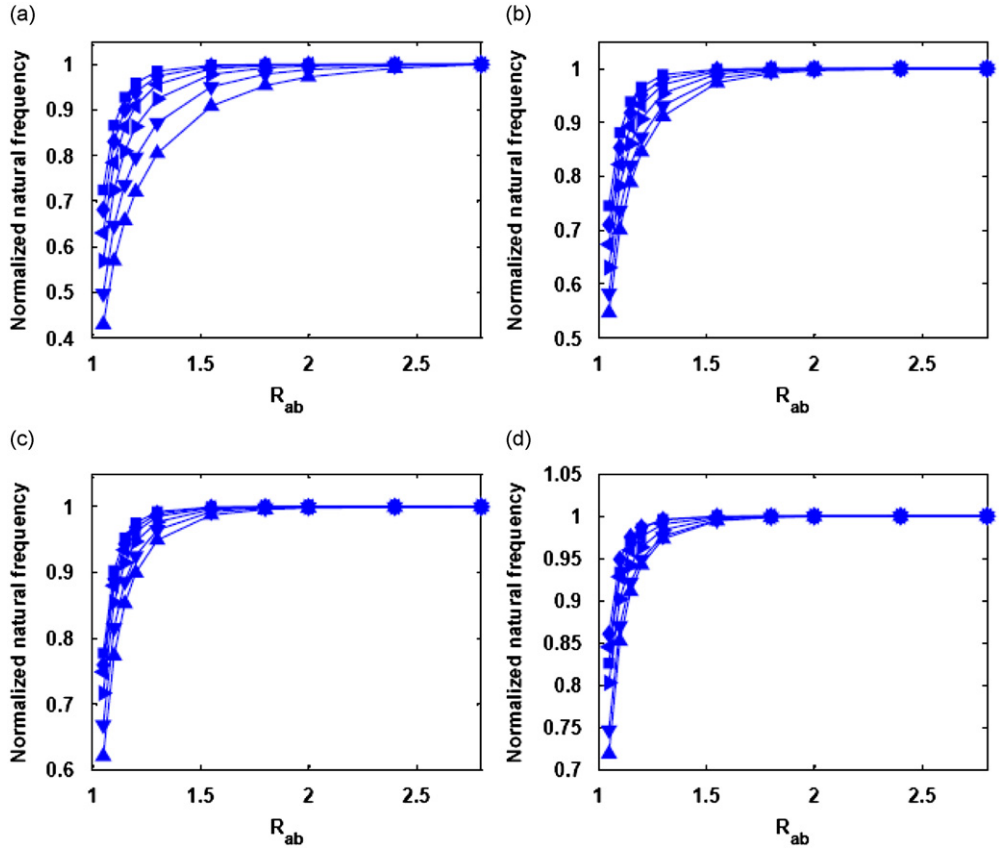

Fig. 6. Normalized natural frequencies of the submerged shell as a function of radius ratio (R_{ab}): (a) first axial half-wave ($m=1$); (b) second axial half-wave ($m=2$); (c) third axial half-wave ($m=3$); (d) fourth axial half-wave ($m=4$) (—▲—, $n=1$; —▼—, $n=2$; —▶—, $n=3$; —◀—, $n=4$; —◆—, $n=5$; —■—, $n=6$).

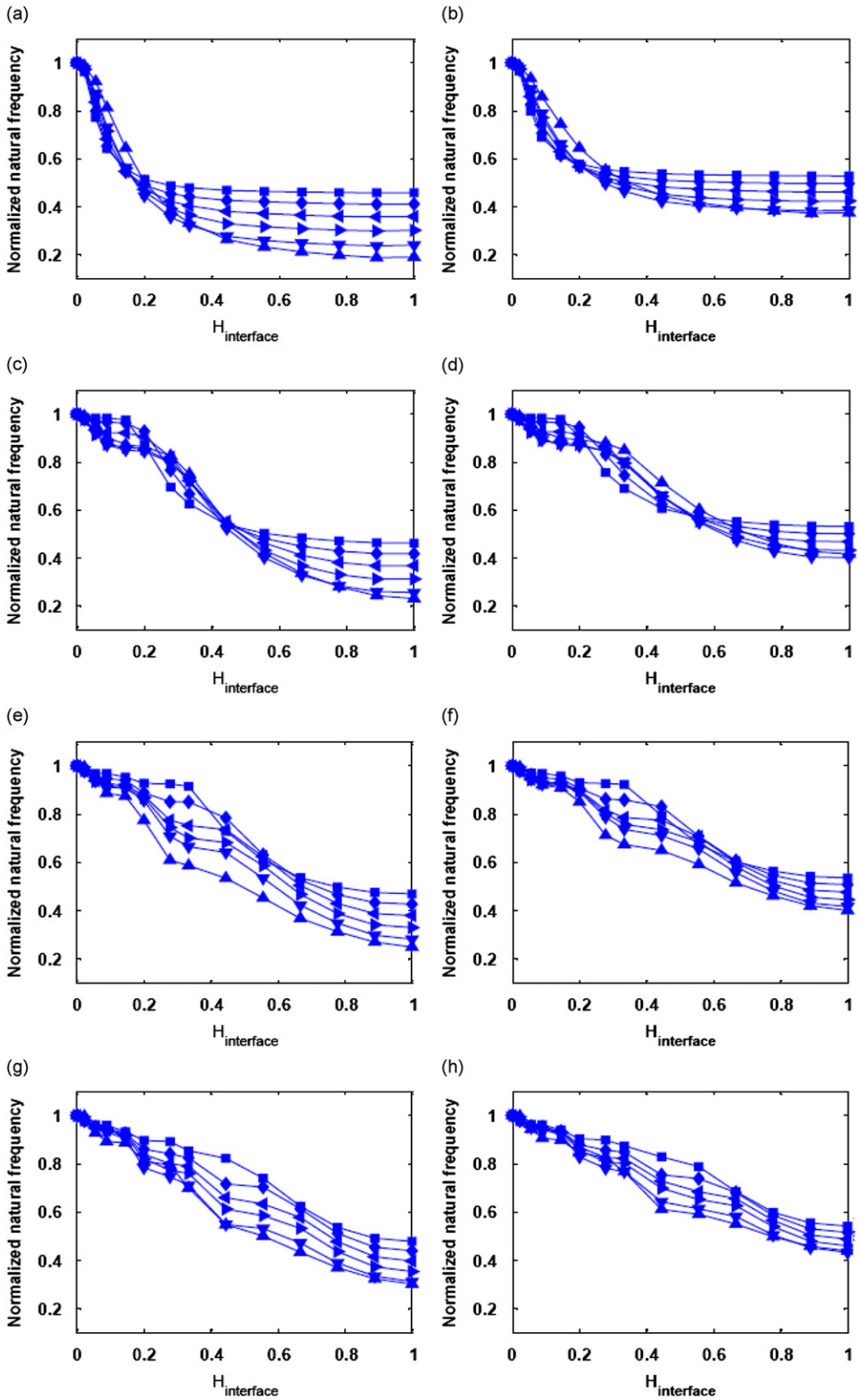

Fig. 7. Effect of submerged ratio on natural frequencies of the submerged shell: (a) first axial half-wave, R_{ab} =1.1; (b) first axial half-wave, R_{ab}=4; (c) second axial half-wave, R_{ab} =1.1; (d) second axial half-wave, R_{ab}=4; (e) third axial half-wave, R_{ab}=1.1; (f) third axial half-wave, R_{ab}=4; (g) fourth axial half-wave, R_{ab}=1.1; (h) fourth axial half-wave, R_{ab}=4 (—▲—, n=1; —▼—, n=2; —▶—, n=3; —◀—, n=4; —◆—, n=5; —■—, n=6).

3.3. Effect of the submergence depth

The submerged ratio is defined as

$$H_{\text{interface}} = \frac{h-(L-H)}{h},\ 0 \le H_{\text{interface}} \le 1 \tag{44}$$

In addition, a normalized natural frequency is defined as the wet natural frequency divided by the in vacuo one of the shell for the specific corresponding mode.

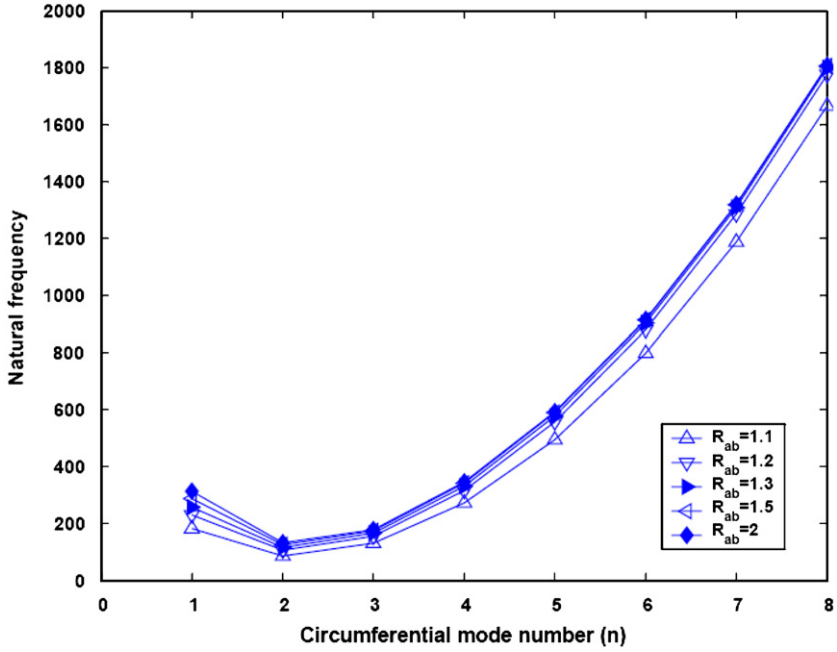

Fig. 8. Normalized natural frequency of the submerged shell with respect to circumferential wavenumber n, for m=1.

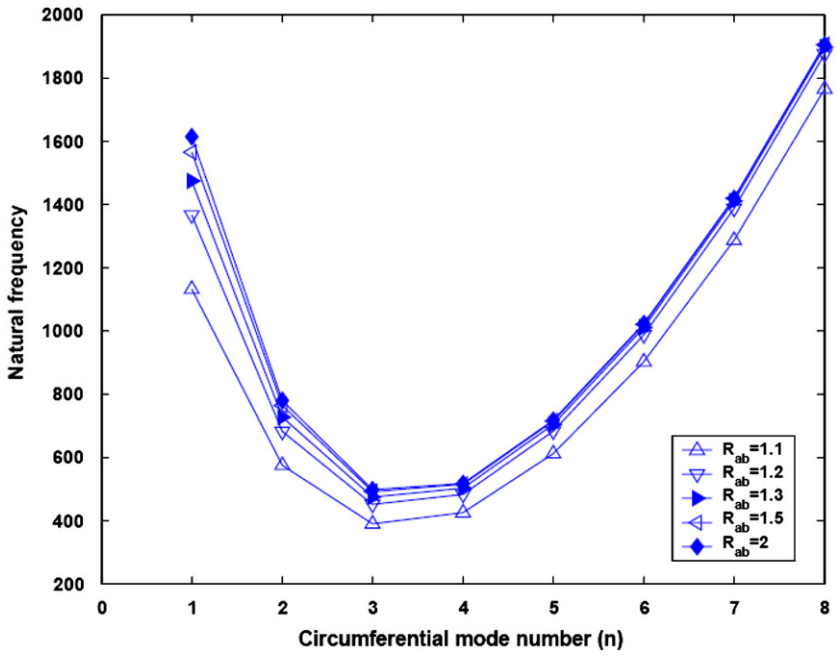

Fig. 9. Normalized natural frequency of the submerged shell with respect to circumferential wavenumber n, for m=2.

Fig. 7 shows the normalized natural frequencies of the submerged cylindrical shell as a function of submerged ratio, $H_{\text{interface}}$. In fact, with increasing the submerged ration, the hydrodynamic mass increases which causes the natural frequencies to decrease. Although the figure shows similar trend for both radius ratios 1.1 and 4, the effect of the submerged ratio on the natural frequencies of the coupled system with radius ratio 4 is less than that those of with radius ratio 1.1. The effect of the submerged ratio on the frequencies of the submerged cylindrical shell is stronger for modes with smaller axial half-wave and circumferential wavenumbers n, m.

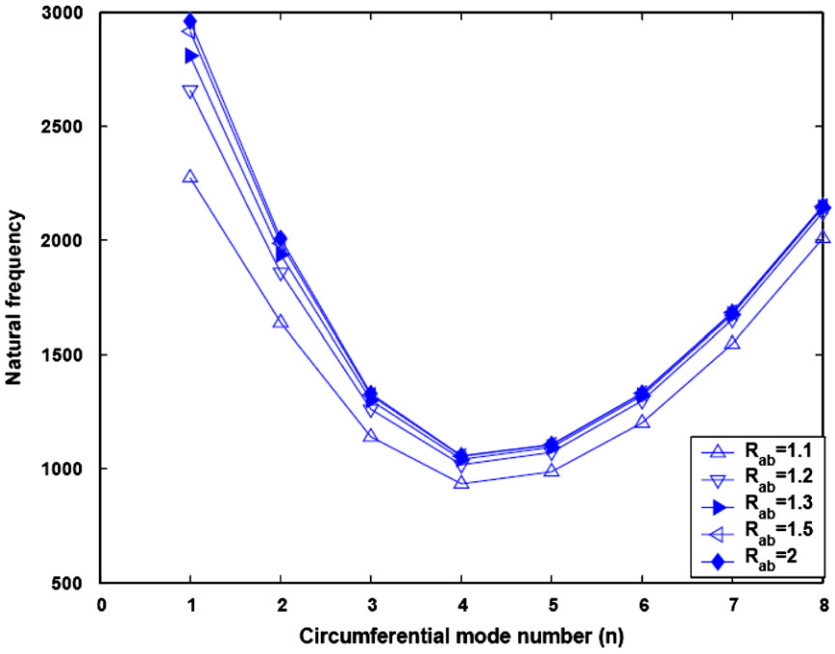

Fig. 10. Normalized natural frequency of the submerged shell with respect to circumferential wavenumber n, for m=3.

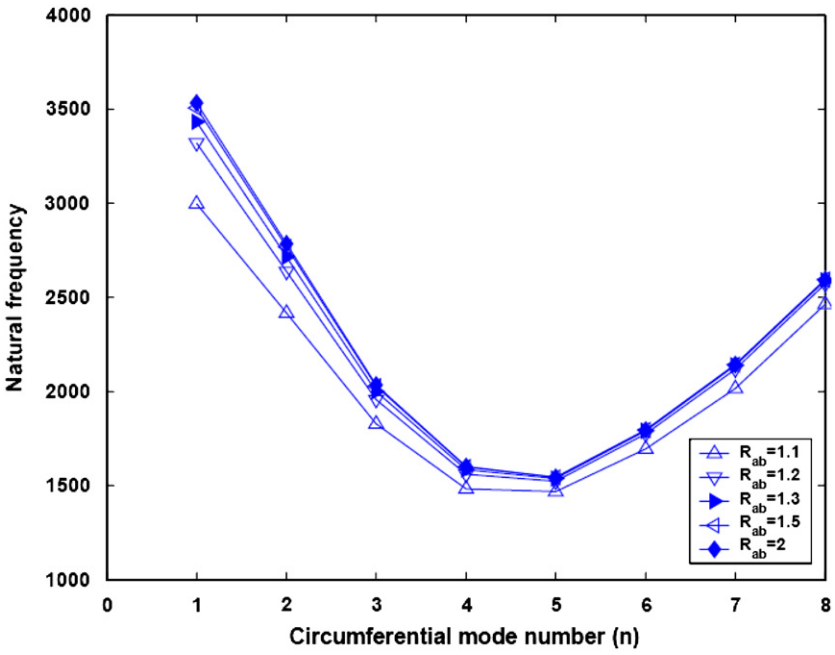

Fig. 11. Normalized natural frequencies of the submerged shell with respect to circumferential wavenumber n, for m=4.

3.4. Effect of the circumferential wavenumber n

The natural frequencies of the submerged cylindrical shell for different circumferential wavenumbers, n, are shown in Figs. 8–11. They are also plotted for different values of m=1–4 and R_{ab}=1.1, 1.2, 1.3, 1.5, and 2.0. As it can be seen from these figures, the minimum natural frequency for each radius ratio occurs at $n=m+1$.

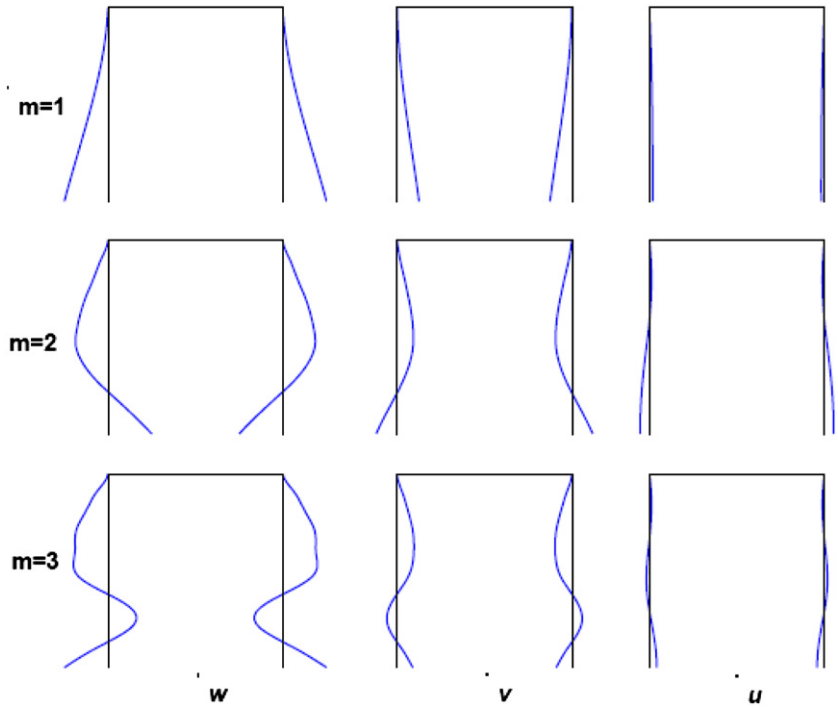

Fig. 12. First three modes having the circumferential wavenumber n=2 in radial w, circumferential v and axial u directions.

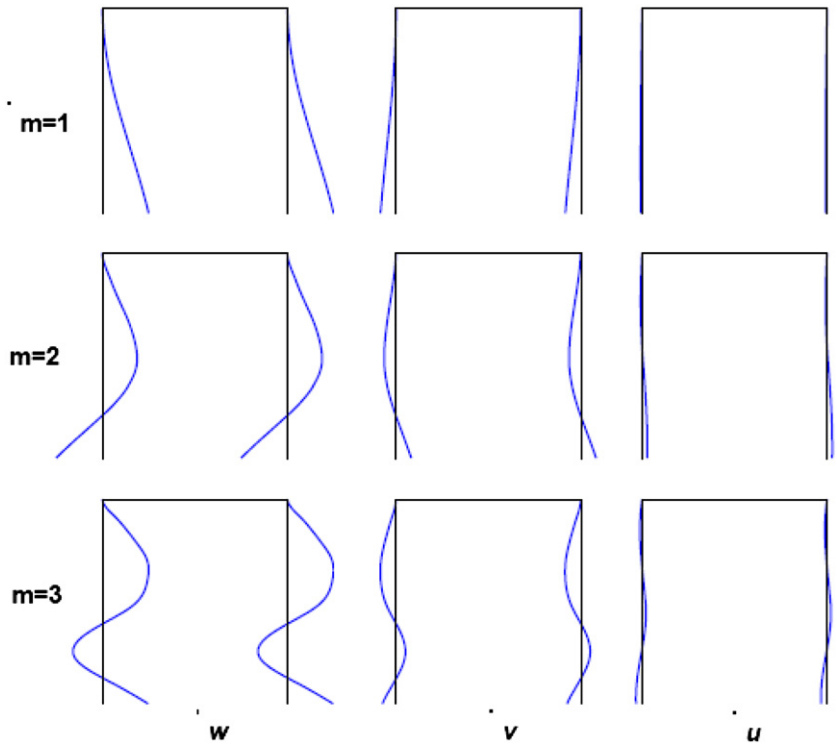

Fig. 13. First three modes having the circumferential wavenumber n=3 in radial w, circumferential v and axial u directions.

3.5. Mode shapes of vibration

The first three mode shapes of the submerged cylindrical shell having the circumferential wavenumber n=2 in radial (w), circumferential (v) and axial (u) direction are given in Fig. 12. Mode shapes are plotted for shell section defined by θ=0 and $\theta=\pi$. Obviously, the mode shapes are symmetric in this case, n=2. The first three mode shapes of the submerged cylindrical shell having n=3 in radial (w), circumferential (v) and axial (u) direction are presented in Fig. 13. As seen in Figs. 12 and 13, the shell displacements in radial direction (w) are larger than shell displacements in other directions (axial and circumferential direction (u, v)). Moreover, the mode shapes for the submerged shell are approximately similar to those for the shell vibrating in air.

The mode shapes of the cylindrical shell for different submerged ratios ($H_{\text{interface}}$) and for n=2, 3 are shown in Figs. 14 and 15, respectively. These mode shapes represent the radial (w) displacement of the shell. As can be observed from these

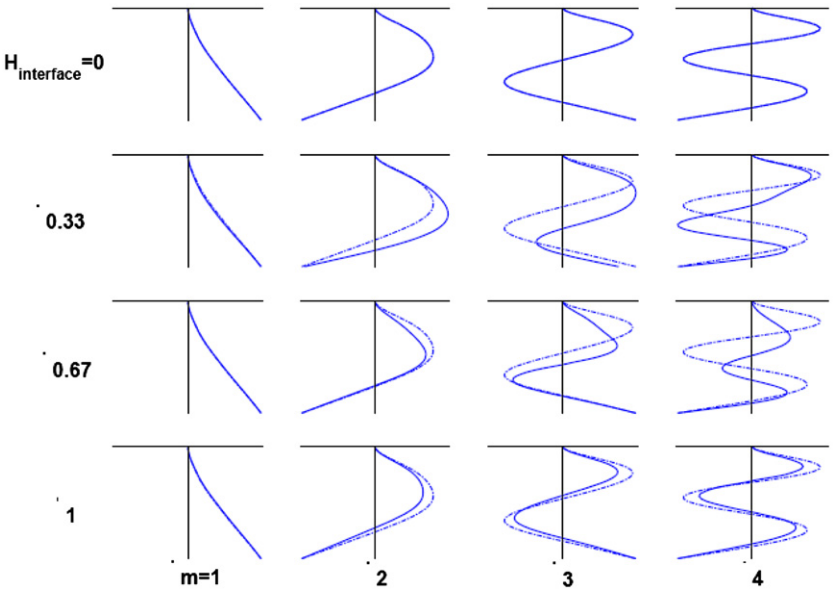

Fig. 14. The variation of the mode shape with variation of submerged ratio ($H_{\text{interface}}$) for circumferential mode number n=2: ——, in water; · · · · · · · · · ·, in air.

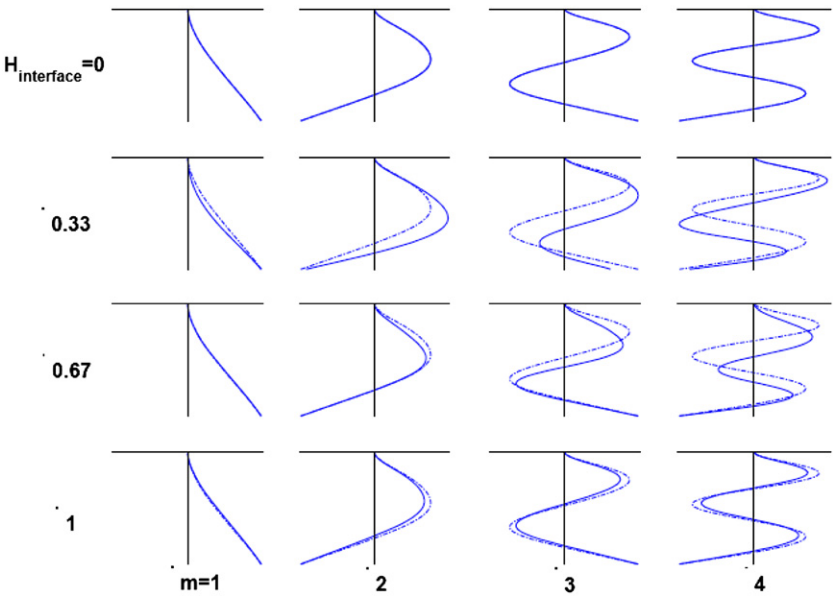

Fig. 15. The variation of the mode shape with variation of submerged ratio ($H_{\text{interface}}$) for circumferential mode number n=3; ——, in water; · · · · · · · · · ·, in air.

figures, the location of the nodal points (the points that are immobile during vibration) changes with the value of submerged ratio. The mode shapes in Figs. 12–15 are normalized with respect to their absolute maximum displacements.

4. Conclusions

The coupled vibration of a cantilever cylindrical shell partially and concentrically submerged in a partially fluid-filled rigid cylindrical container was considered. The developed method captures the analytical features of the velocity potential in a continuous, simply connected and non-convex fluid domain including the interaction between the fluid and the internal body. The possibility of testing and analyzing different sizes of system variables that affect the dynamic characteristics of the partially submerged cylindrical shell may be considered as an advantage of the present method. It should also be noted that using the analytical method proposed in the present paper allows a fast and reliable solution to the problem for large container radius, a, when compared with some numerical solutions, e.g., finite element method. It is in agreement with the conclusion mentioned by Amabili [18] "An unbounded fluid domain, such as the one studied, can be simulated with difficulty by standard finite element programs. In contrast, the Rayleigh–Ritz method, employed in the present study, allows a first and reliable solution to the problem to be obtained."

In order to evaluate the dynamic characteristics of the coupled system, the effects of submergence depth, axial and radial distances between the cylindrical shell and the cylindrical container, and the circumferential wavenumber n on the natural frequencies and mode shapes of the coupled system were investigated. It was found that by increasing the submergence depth, the natural frequencies of the submerged shell decrease. It was also obtained that an increase of axial distance between the shell and the container produces an increase of the natural frequencies. The natural frequencies of the submerged shell increase with increasing radial distance between the shell and the container. The effect of submergence depth, axial and radial distance between the shell and the container on the coupled system varies with axial half-wave and circumferential wavenumbers (m, n), i.e., this effect was stronger for modes with smaller axial half-wave and circumferential wavenumbers.

The developed analytical method was verified by FEM results, the results of which show excellent agreement. This method can be extended to the fluid–structure interaction problems involving different shapes of the flexible internal body.

References

[1] D.V. Evans, P. McIver, Resonant frequencies in a container with a vertical baffle, *Journal of Fluid Mechanics* 175 (1987) 295–307.
[2] E.B.B. Watson, D.V. Evans, Resonant frequencies of a fluid in containers with internal bodies, *Journal of Engineering Mathematics* 25 (1991) 115–135.
[3] I. Gavrilyuk, I. Lukovsky, Yu. Trotsenko, A. Timokha, Sloshing in a vertical circular cylindrical tank with an annular baffle. Part 1. Linear fundamental solutions, *Journal of Engineering Mathematics* 54 (2006) 71–88.
[4] S. Mitra, K.P. Sinhamahapatra, Slosh dynamics of liquid-filled containers with submerged components using pressure-based finite element method, *Journal of Sound and Vibration* 304 (2007) 361–381.
[5] A. Maleki, M. Ziyaeifar, Sloshing damping in cylindrical liquid storage tanks with baffles, *Journal of Sound and Vibration* 311 (2008) 372–385.
[6] J.R. Cho, H.W. Lee, K.W. Kim, Free vibration analysis of baffled liquid-storage tanks by the structural-acoustic finite element formulation, *Journal of Sound and Vibration* 258 (5) (2002) 847–866.
[7] A. Ergin, B. Ugurlu, Linear vibration analysis of cantilever plates partially submerged in fluid, *Journal of Fluids and Structures* 17 (2003) 927–939.
[8] K.C. Biswal, S.K. Bhattacharyya, P.K. Sinha, Dynamic response analysis of a fluid-filled cylindrical tank with annular baffle, *Journal of Sound and Vibration* 274 (2004) 13–37.
[9] M. Esmailzadeha, A.A. Lakis, M. Thomas, L. Marcouiller, Three-dimensional modeling of curved structures containing and/or submerged in fluid, *Finite Elements in Analysis and Design* 44 (2008) 334–345.
[10] Y. Kerboua, A.A. Lakis, M. Thomas, L. Marcouiller, Vibration analysis of rectangular plates coupled with fluid, *Applied Mathematical Modelling* 32 (12) (2008) 2570–2586.
[11] M. Amabili, G. Dalpiaz, Vibrations of base plates in annular cylindrical tanks: theory and experiments, *Journal of Sound and Vibration* 210 (3) (1998) 329–350.
[12] H.J.P. Morand, R. Ohayon, *Fluid–Structure Interaction, Applied Numerical Methods*, Wiley, New York, 1995.
[13] A.E.H. Love, *A Treatise on the Mathematical Theory of Elasticity*, first ed., Cambridge University Press, 1892; fourth ed., Dover Publications, Inc., New York, 1944.
[14] Y.W. Kim, Y.S. Lee, S.H. Ko, Coupled vibration of partially fluid-filled cylindrical shells with ring stiffeners, *Journal of Sound and Vibration* 276 (2004) 869–897.
[15] W. Soedel, *Vibrations of Shells and Plates*, second ed., Marcel Dekker, New York, 2003.
[16] Y.S. Lee, Y.W. Kim, Effect of boundary conditions on natural frequencies for rotating composite cylindrical shells with orthogonal stiffeners, *Advances in Engineering Software* 30 (1999) 649–655.
[17] R.D. Blevins, *Formulas for Natural Frequency and Mode Shapes*, Van Nostrand Reinhold Company, London, 1979.
[18] M. Amabili, Vibrations of circular tubes and shells filled and partially immersed in dense fluids, *Journal of Sound and Vibration* 221 (4) (1999) 567–585.
[19] M. Amabili, Eigenvalue problems for vibrating structures coupled with quiescent fluids with free surface, *Journal of Sound and Vibration* 231 (1) (2000) 79–97.
[20] F. Zhu, Rayleigh quotients for coupled free vibrations, *Journal of Sound and Vibration* 171 (1994) 641–649.
[21] M. Amabili, Ritz method and substructuring in the study of vibration with strong fluid–structure interaction, *Journal of Fluids and Structures* 11 (1997) 507–523.
[22] O.C. Zienkiewicz, *The Finite Element Method*, McGraw-Hill Company, London, 1997.
[24] M. Ohkusu, Hydrodynamic forces on multiple cylinders in waves, *Proceedings of the International Symposium on Dynamics of Marine Vehicles and Structures in Waves*, Vol. 90, London, Institute of Mechanics, 1970, pp. 337–362.
[25] M.A. Srokosz, D.V. Evans, A theory for wave-power absorption by two independently oscillating bodies, *Journal of Fluid Mechanics* 90 (1979) 337–362.